Pergamon

PII: S0301-9322(96)00039-0

Int. J. Multiphase Flow Vol. 22, No. 6, pp. 1143–1154, 1996

0301-9322/96 $15.00 + 0.00

AN EXPERIMENTAL STUDY ON DEVELOPING AIR–WATER TWO-PHASE FLOW ALONG A LARGE VERTICAL PIPE: EFFECT OF AIR INJECTION METHOD

A. OHNUKI and H. AKIMOTO

Japan Atomic Energy Research Institute, Tokai-mura, Ibaraki-ken 319-11, Japan

(Received 1 September 1995; in revised form 15 May 1996)

Abstract—The flow structure in a developing air–water two-phase flow was investigated experimentally along a large vertical pipe (inner diameter, D_h: 0.48 m, ratio of length of flow path L to D_h: about 4.2). Two air injection methods (porous sinter injection and nozzle injection) were adopted to realize an extremely different flow structure in the developing region. The flow rate condition in the test section was as follows: superficial air velocity: 0.02–0.87 m/s (at atmospheric pressure) and superficial water velocity: 0.01–0.2 m/s, which covers the range of bubbly to slug flow in a small-scale pipe ($D_h \leq$ about 0.05 m).

No air slugs occupying the flow path were recognized in this experiment regardless of the air injection methods even under the condition where slug flow is realized in the small-scale pipe. In the lower half of the test section, the axial distribution of sectional differential pressure and the radial distribution of local void fraction showed peculiar distributions depending on the air injection methods. However, in the upper half of the test section, the effects of the air injection methods are small in respect of the shapes of the differential pressure distribution and the phase distribution. The comparison of sectional void fraction near the top of the test section with Kataoka's correlation indicated that the distribution parameter of the drift–flux model should be modeled including the effect of D_h and the bubble size distribution is affected by the air injection methods. The bubble size distribution is considered to be affected also by L/D_h based on comparison of results with Hills' correlation. Copyright © 1996 Elsevier Science Ltd.

Key Words: gas–liquid two-phase flow, large diameter, vertical pipe, developing flow, bubbly flow, void fraction, phase distribution, drift–flux model

1. INTRODUCTION

In recent years, postulated accidents in light water reactors are analyzed by the so-called best-estimate codes like TRAC and RELAP5 (Ross 1988). The best-estimate code is based on a two-fluid model with flow-regime-dependent constitutive equation treatment. The two-fluid model code is one of the most advanced analytical tools and is expected to be used for the calibration of licensing codes and the design of advanced light water reactors. However, the predictive accuracy of the code strongly depends on whether or not the applicability of physical models in the constitutive equations is verified for the fluid condition and geometry in a specific problem because most of the physical models have some empirical factors.

Most of the hydraulic models in the constitutive equations including flow pattern map have been derived from relatively small-scale experiments and under a fully developed flow condition (Liles *et al.* 1988). Typical dimensions of the experiments were that the hydraulic diameter D_h of flow path was less than about 0.05 m and the ratio of length of flow path L to D_h was more than about 100. However, in an actual reactor, the range of the hydraulic diameter D_h is from about 0.01 m to about 1 m and the ratio of L/D_h also have a wide range. This means that it is necessary to assess the physical models for the gas–liquid two-phase flow in a large D_h geometry and under a developing flow condition in a small L/D_h region in order to quantify the predictive accuracy of the two-fluid model code to an actual reactor. However, the data-base for such geometry and flow condition is not adequate for assessing the hydraulic models. Flow pattern map, pressure loss and void fraction in the flow path are at least needed as the data-base for assessing an one-dimensional two-fluid model and the distributions of phase and velocity in the axial and the radial directions of the flow path are further required for a multidimensional two-fluid model.

For a large vertical flow path, Kataoka & Ishii (1987) summarized previous studies (D_h: 0.011–0.61 m, fluid: air–water, air–glycerine and steam–water, pressure: 0.101–18.2 MPa) and developed a new drift–flux type correlation for pool void fraction. Under bulk liquid flow condition in air–water two-phase flow, Hills (1976) proposed a correlation for average void fraction in a vertical flow path with D_h of 0.15 m (L/D_h: 70) and Hashemi *et al.* (1986) investigated the flow pattern and void fraction in a specific geometry with D_h of 0.1 m (L/D_h: 30) or 0.3 m (9.5), the geometry which simulated once-through steam generators of Babcock & Wilcox (B&W) pressurized water reactor, i.e. a horizontal inlet pipe connected to a vertical pipe via an elbow with a bend at the vertical pipe exit. From these studies, the data-base for the average void fraction is supposed to be enough while effects of the bulk liquid flow have not been investigated in steam–water system. However, effects of the mixing methods of gas and liquid are considered to be important for the large D_h and small L/D_h geometry but studies on the developing flow are scarce. Hills reported that the length of the developing flow region became longer with increasing liquid flow rate, but the effects of mixing methods and gas flow rate were not reported. Ueyama *et al.* (1980) investigated a developing flow in a bubble column (D_h: 0.6 m) using two different air injection nozzles. They reported that the length of the developing flow was influenced by the absolute value of water depth, but the effects of the mixing methods were not fully examined. Furthermore, studies on flow structure (phase and velocity distribution) including the flow pattern also scarcely exist.

Hills made a flow pattern map including a slug flow. Hashemi *et al.* reported that a slug flow was realized in the flow path with D_h of 0.1 m but no slug bubbles existed in the flow path with D_h of 0.3 m while some large bubbles were observed. Kataoka & Ishii supposed from an instability analysis that a large bubble disintegrates to cap bubbles and no slug flow is realized in a flow path with about 0.1 m D_h in an air–water system under room temperature condition. Ueyama *et al.* reported that cross-sectional average of volume–surface mean diameter of bubbles was at around 0.01 m in the bubble column of 0.6 m i.d. We performed an air–water experiment with a large vertical pipe which L/D_h is relatively small (D_h of 0.48 m and L/D_h of about 4.2) (Ohnuki *et al.* 1995). No air slugs occupying the flow path were recognized in our experiment even under the condition where the slug flow is realized in a small-scale pipe and the churn bubbly flow was observed under the condition. It is considered from these studies that a slug flow occupying flow path is not able to be sustained due to an interfacial instability in the flow path with D_h more than 0.3 m. However, in the experiments by Hashemi *et al.*, a separated two-phase flow run through a horizontal inlet pipe and flowed into a vertical pipe via an elbow. It showed in the flow pattern sketch in their paper that a large bubble, which generated at the elbow, flowed into the vertical section and disintegrated to smaller bubbles. This mixing configuration is peculiar and it is not clear whether or not the data are also applicable to another geometries like upper plenum in reactor pressure vessel. Our experiment used a porous sinter wall to inject air and it was not clarified whether the disappearance of slug flow in the large vertical pipe also occurs under another air injection methods.

In this study, we investigate experimentally the flow structure in a developing air–water two-phase flow along a large vertical pipe which L/D_h is relatively small (D_h of 0.48 m and L/D_h of about 4.2). As the mixing methods, two extremely different air injection methods are adopted in this experiment. One method uses a porous sinter wall to inject air that is the same as the previous study (Ohnuki *et al.* 1995) and the other uses a nozzle with inner diameter of 0.07 m for the air injection. By using the two methods, effects of the size of injected air bubbles can be examined along the large vertical pipe. The measurement items are the flow pattern, the axial distribution of sectional differential pressure and the radial distribution of local void fraction. The sectional average void fraction near top of test section will be compared with the previous correlations (drift–flux type Kataoka's correlation and Hills' correlation which gives the relation between the relative velocity between phases, V_r, and the void fraction, ϵ).

2. EXPERIMENT

Figure 1 shows the outline of the experimental rig used in this study. The experimental rig is composed of a test section, an upper plenum located above the test section, a lower plenum under the test section and the air and water sources. The test section is made of a transparent acrylic

resin to observe the flow pattern. D_h and L of the test section are 0.48 and 2 m, respectively. An extension pipe of 0.75 m length which is made of stainless steel is attached on the test section. The upper and the lower plenums are made of stainless steel and the dimensions are inner diameter: 1 m and height: about 1 m. The lower plenum can set up an air injection device inside the plenum which is a porous sinter tube (grain size: 50 μm) or a nozzle of 0.07 m inner diameter. The porous sinter tube is a rectangular shape in the cross section and the top view of the tube is a foursquare ring. The outer dimension of the ring is 0.37 × 0.37 m and the inner one is 0.28 × 0.28 m. The height of the tube is 0.04 m. Porous sinter walls are equipped at side walls of the rectangular ring and the top and the bottom walls are solid one. In the case of using the nozzle device, the top of nozzle is located at the center of the test section bottom.

The air was fed from compressors via an orifice flow meter to the air injection devices. The water was injected into the bottom of the lower plenum via an electromagnetic flow meter. The water temperature was kept to be constant, about 35°C, by a cooler to remove heat from a pump. The top of the upper plenum is open to the atmosphere.

The experimental conditions for air and water flow rates were as follows: superficial air velocity in the test section (j_G): 0.02–0.87 m/s (at atmospheric pressure); and superficial water velocity in the test section (j_L): 0.01–0.2 m/s.

The maximum error for each flow rate was estimated as ±1% of the flow rate which was caused by the uncertainty of differential pressure measurements or that of the electromagnetic flow meter.

Measurement items in this study were as follows:

(1) flow pattern by a high speed video system (200 frames/s) and still pictures,
(2) differential pressure at six axial sections of the test section as shown in figure 1 and
(3) local void fraction by an optical void probe (KANOMAX Japan (Ltd) System 7933).

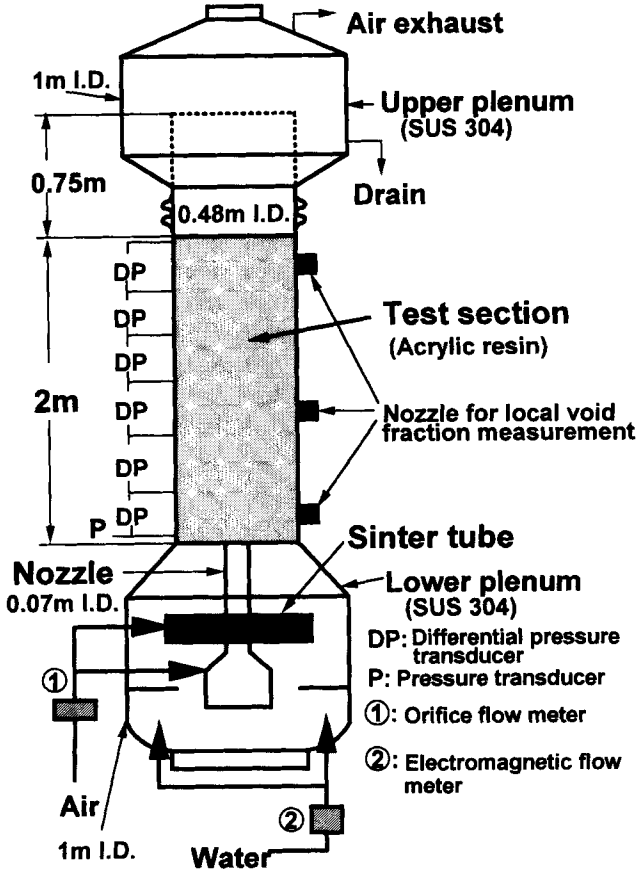

Figure 1. Schematic of experimental rig.

The span for the differential pressure measurements was from 0.2 to 0.47 m and the maximum error was estimated as ± 0.1 kPa/m which was caused by the uncertainty of the differential pressure measurements.

The light source of the optical void probe is 2 mW He–Ne laser and the light emitted at the source is transmitted through an optical fiber. The outer diameter of the tip of the optical probe is 0.35 mm. The transmitted light is reflected at the tip. The optical probe used in this study is L type and the orientation in the test section is vertically downward. The probe meter can produce a signal with a level depending on the phase (gas or liquid) at the probe tip because the amplitude of the reflected light in the case of gas is different from that in the case of liquid. We processed the signal to convert to the local void fraction by counting the time spent in the gas state over the total time.

3. RESULTS AND DISCUSSION

In order to investigate the flow structure in a developing air–water two-phase flow along the large vertical pipe, the following results on effects of the air injection methods are shown and discussed: (1) flow pattern, (2) axial distribution of differential pressure, (3) radial distribution of local void fraction and (4) average sectional void fraction at the top region of the test section which was estimated from the sectional differential pressure measurement by neglecting accelerative and frictional pressure losses. In this paper, the air injection methods with devices of the porous sinter tube and the nozzle are called sinter injection and nozzle injection, respectively.

3.1. Flow pattern

The flow pattern was basically changed from an uniform bubbly flow to a churn bubbly flow with increasing J_G at a fixed J_L while it was observed in the nozzle injection that a large bubble at the nozzle exit disintegrated to smaller bubbles along the lower half of the test section. Figure 2 compares typical flow patterns in the upper half of the test section at different J_G condition. In the lower part of figure 2, all experimental conditions in this study are shown in the map of $J_G - J_L$. The classification of the flow pattern as uniform, agitated and churn bubbly flows was derived for the sinter injection in the previous study (Ohnuki *et al.* 1995). The corresponding conditions for A, B and C are indicated in the map. The boundary between bubbly and slug flows by Mishima & Ishii (1984) is also included in the map.

In the sinter injection, an uniform bubbly flow where bubbles flow upwards with no significant fluctuation can be observed in the condition A. We call the flow pattern as the uniform bubbly flow. In the conditions B and C, some large eddies including bubble clusters fill up the flow path. It was found from the flow observation by the high speed video system that the flow direction of a cluster was random due to a large eddy and the random movement of the clusters agitated the bubbly flow pattern. It was also recognized from the video image that the large eddies flowed so as to twine one another and the flow was unstable and oscillatory. Some bubble clusters with downward flow direction was frequently observed. The downward flow became significant with increasing J_G. We call the flow pattern in the condition C as the churn bubbly flow. In the condition B, the bubbly flow pattern was agitated due to random movement of the bubble clusters but the flow oscillation was calmer than that under the condition C. We call the flow pattern in the condition B as the agitated bubbly flow. The boundaries between the uniform and the agitated bubbly flows and between the agitated and the churn bubbly flows were determined by the flow observation and by the magnitude of the standard deviation of sectional void fraction fluctuation, respectively, as described in the previous study (Ohnuki *et al.* 1995).

In the nozzle injection, almost the same flow patterns were observed except for the region of the disintegration of large bubbles in the lower half of the test section. But some clusters of bubbles were observed in the condition A and some cap-bubbles were recognized. Non-uniform distribution of bubbles can be observed in the condition A of the nozzle injection in figure 2. Since no large bubbles like cap-bubble were recognized in the sinter injection, the existence of cap-bubbles in the nozzle injection indicates that the initial bubble size at the test section inlet affects the bubble size distribution along the test section.

Although a slug flow is realized in a small-scale flow path ($D_h \leqslant$ about 0.05 m) in the condition C based on the proposed criterion by Mishima–Ishii, there were no slug bubbles occupying the

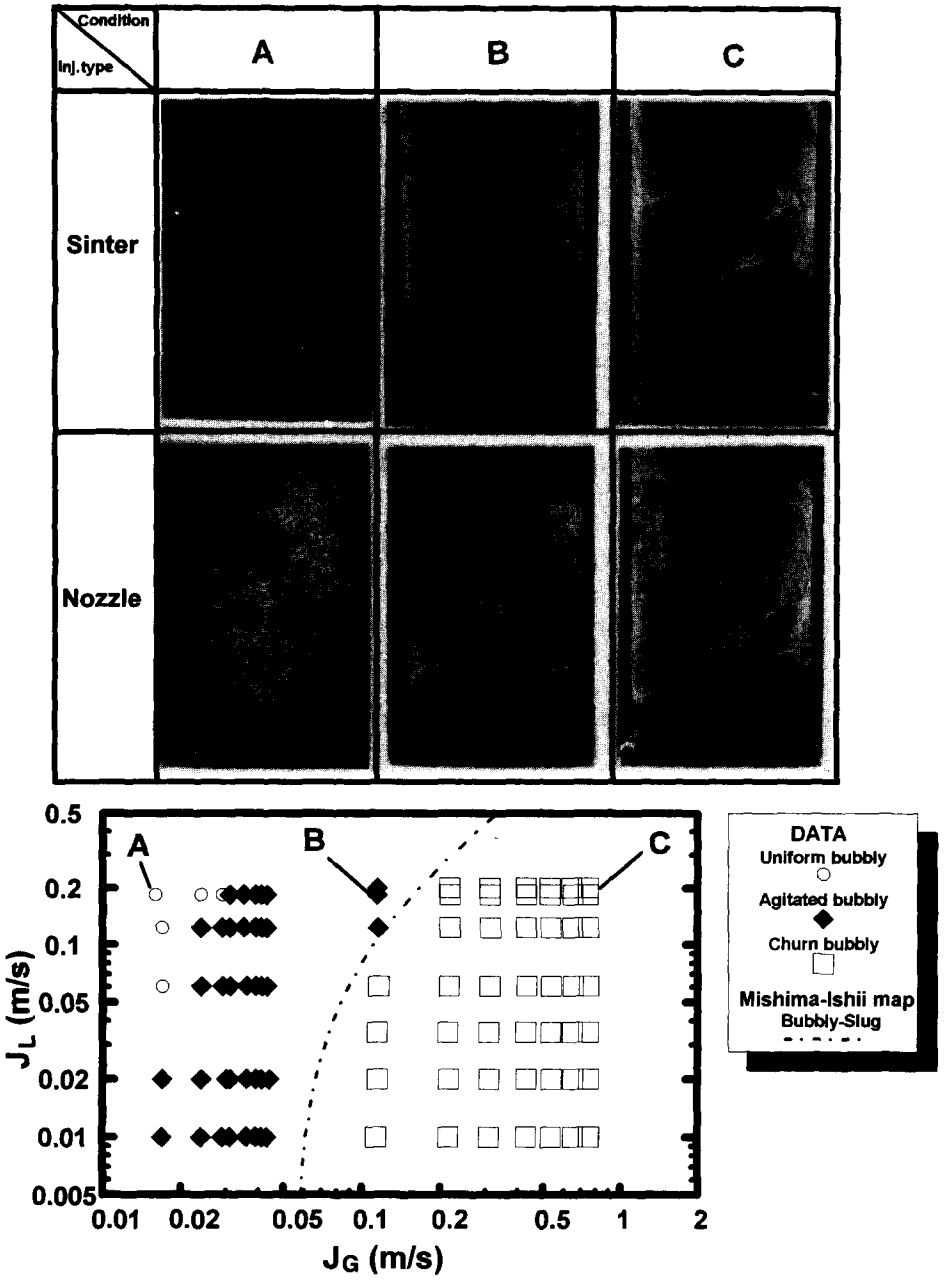

Figure 2. Comparison of flow pattern in upper half of test section (black arrow near the center in upper half of test section is a marker (3 × 15 cm)).

flow path under the condition in this study. In the slug flow region in the map of figure 2, an unstable and oscillatory behaviors of bubble clusters were observed in this study. The observation results in this study indicate that it is difficult to sustain a large slug bubble in the large vertical pipe even under the condition that a slug flow is established in a small-scale flow path. The interfacial instability was clearly recognized by the flow observation in the nozzle injection that a large bubble at the test section inlet disintegrates to smaller bubbles along the lower half of the test section.

3.2. Differential pressure distribution along test section

Figures 3 and 4 compare the differential pressure along the test section in respect of effects of J_G under the same J_L and of J_L under the same J_G, respectively. Each differential pressure value

is time-averaged one. The differential pressure tends to decrease with increasing J_G or with decreasing J_L while the tendency is not recognized in the case of $J_G = 0.13$ m/s in figure 4(a) and at the lower half in $J_G = 0.82$ m/s in figure 4(a). The effect of J_G on the differential pressure is larger than that of J_L within the experimental condition in this study.

In the sinter injection, the axial distribution becomes a nonuniform with increasing J_G and the differential pressure below the middle height of the test section becomes lower than that above the middle height. The lower differential pressure is considered to be caused by effects of a developing flow. One of possible reasons is that a pressure recovery due to deceleration of water because the degree of acceleration of water by air bubbles near the porous sinter wall is considered to become higher with increasing J_G and the accelerated water decelerates to an equilibrium condition along the test section.

In the nozzle injection, the differential pressure near the bottom of test section almost equals to the differential pressure of single-phase water that is about 10 kPa/m. The differential pressure gradually decreases towards the middle height of test section and the distribution of differential pressure is almost flat in the upper half of test section. The differential pressure in the upper half of test section is slightly higher than that in the sinter injection under the same J_G and J_L conditions. In the nozzle injection, air was injected intermittently as a large bubble at the bottom center of the test section and the large bubble disintegrated to smaller bubbles along the lower half of the test section as described in the previous section. The distribution of differential pressure along the test section is considered to be related to the disintegration of the large bubble. From the flow observation by high speed video, it was found that the large bubble had a high rising velocity and disintegrated to smaller bubbles with lower velocity. Since the lower relative velocity gives a higher void fraction, the decrease of differential pressure along the lower half of test section can be explained by the difference of the relative velocity between the large bubble and the smaller bubbles.

The distribution of differential pressure along the test section is almost uniform in the upper half of test section regardless of the air injection methods. This might indicate that the two-phase flow almost reaches a developed condition at the middle height of the test section, i.e. about 1 m height. Ueyama *et al.* (1980) measured the axial distribution of sectional void fraction in the bubble column

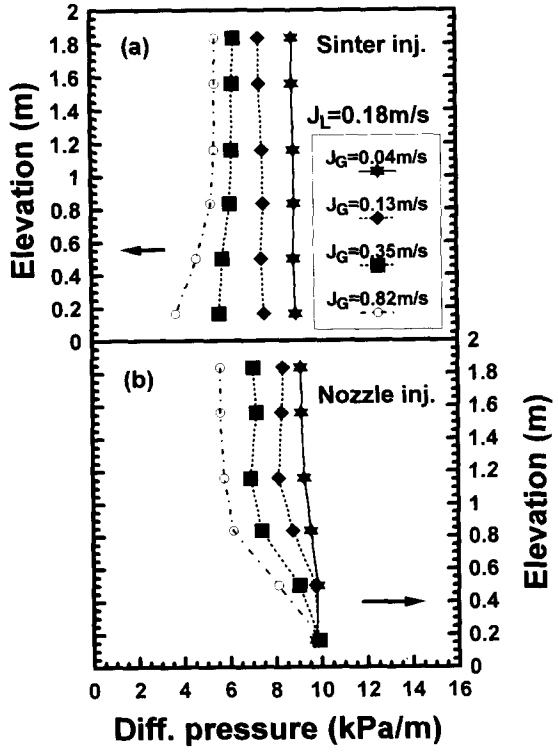

Figure 3. Comparison of differential pressure along test section under different J_G ((a) air injection with sinter pipe, (b) air injection with nozzle).

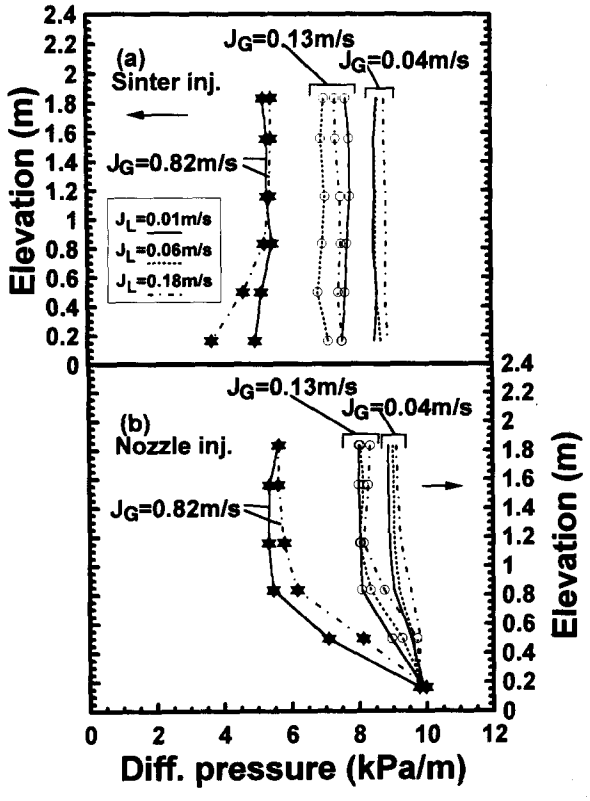

Figure 4. Comparison of differential pressure along test section under different J_L ((a) air injection with sinter pipe, (b) air injection with nozzle).

(D_h: 0.6 m). Most of the data in their paper were derived using the multi-nozzle air injector which consists of 16 nozzles of 6 mm i.d. The multi-nozzle was equipped at the bottom of the column being a conical shape of 0.5 π rad cone angle and the air was injected through the nozzle towards the center of the column. Their experimental results showed a similar distribution to that of the nozzle injection of this study and the axial distribution was almost flat above about 1 m height under the froth level higher than about 2 m. These results of the bubble column and the present study indicate that a developing flow is dominant in the region of L/D_h lower than about 2 regardless of the air injection methods. However, more detailed measurements such as measurements of phase distribution along the test section are needed to confirm the length of the developing flow region.

3.3. Phase distribution along test section

Figure 5 shows the variation of phase distribution along the test section. r is the radial position measured from the center and R is the radius of the flow path. The locations of $L/D_h = 0.23$ and 3.82 correspond to the bottom and the top axial regions, respectively, and $L/D_h = 1.74$ corresponds to the middle region. Flow rate condition is the maximum one in this study. The phase distribution in the region of r/R more than 0.9 is not plotted because the measurement in the region is considered to have an uncertainty. As described in section 3.1, a downward bubble motion was frequently observed under a higher J_G. Since the orientation of the local void probe used in this study is vertically downward, an underestimation of void fraction might be occurred when the bubble comes from behind the probe. As shown in the previous study (Ohnuki *et al.* 1995), a liquid downward flow was measured near the wall which was in the range from about 0.9–1.0 in r/R under the condition in this study. Thus, the local void fraction in r/R more than 0.9 is not compared in this section.

The phase distribution near the bottom of test section is distorted due to the location of the air injection devices, i.e. the void fraction at $r/R = 0.55$ is higher than that at the center ($r/R = 0$) in the sinter injection and no air bubbles are existed in the region of r/R more than about 0.6 in the

nozzle injection. The void fraction at the center is lower than that at $r/R = 0.25$ near the bottom of test section in the nozzle injection. This is because an injected large bubble immediately changes to a doughnut-shape large bubble. This change was confirmed by the flow observation with high speed video system. In the case of lower J_G condition, the void fraction at the center was always higher than that at the other location in the nozzle injection because the transition to the doughnut-shape bubble was not observed under the condition.

The phase distribution at the middle and the top regions shows similar shape, i.e. convex shape, regardless of the air injection methods. In the sinter injection, the value of void fraction is almost the same each other and the flow is considered to be almost developed. In the nozzle injection, the void fraction at the middle region is lower than that at the top region and the effect of a developing region is considered to be still remained.

The tendency developing the phase distribution along the bubble column by Ueyama *et al.* (1980) is similar to that of the nozzle injection of this study under a lower J_G condition. A convex shape was also attained at about 0.8 m height under the froth level higher than about 2 m. Although the length of a developing flow in their experiment is not possible to be defined because of lack of measurements of phase distribution at a higher elevation, it can be pointed out from their results and the present work that the phase distribution becomes to a convex shape along the large vertical pipe regardless of the air injection methods.

Figure 6 shows the effect of the air injection method on the phase distribution near the top of the test section. The void fraction in the region of r/R more than about 0.2 is slightly higher in the sinter injection than that in the nozzle injection. However, the shape of phase distribution is similar and the effect of air injection methods is small on the phase distribution near the top of the test section. The slight difference of the void fraction results in the difference of average sectional void fraction at the top of the test section as will be discussed in the next section.

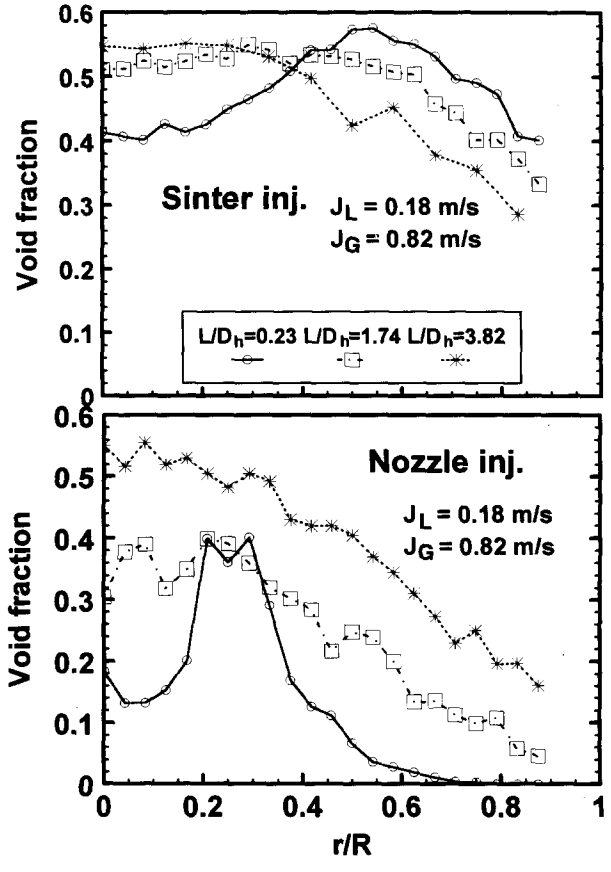

Figure 5. Comparison of phase distribution along test section.

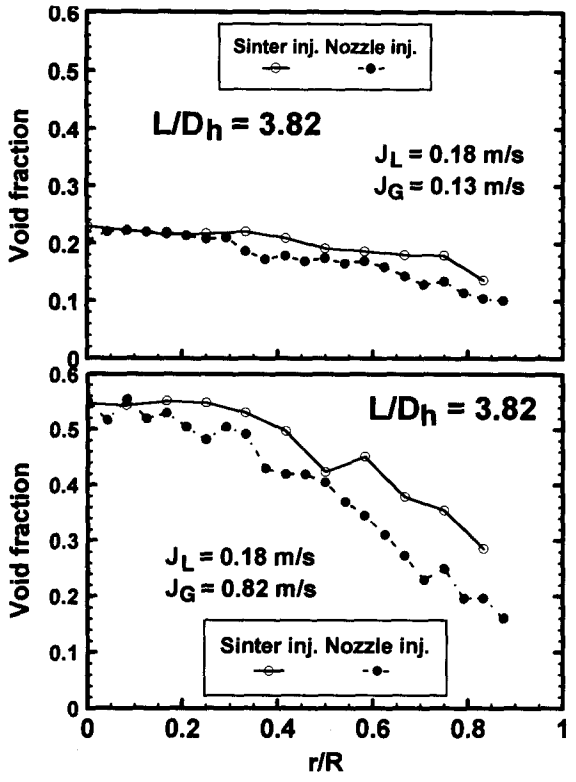

Figure 6. Comparison of phase distribution near top of test section.

3.4. Average void fraction at top of test section

In this section, the characteristics of average void fraction in the large vertical pipe of this study are investigated using previous correlations. Since the void fraction was derived from the sectional differential pressure measurement by neglecting accelerative and frictional pressure losses, the void fraction in the lower half of the test section is difficult to evaluate with good accuracy because the effect of the developing flow is considered to be significant as discussed in the previous sections. Therefore, the data of sectional average void fraction at the top of the test section are used in this section.

Figure 7 shows the drift-flux type relation for all the data in this study and compares with Kataoka & Ishii (1987) correlation. The J_G/ϵ value at $J_G + J_L = 0$ represents the drift velocity V_{Gj} if the distribution parameter C_0, which is the gradient of each line, is assumed to be constant. C_0 was estimated to be about 1.8 for both air injection methods using the least squares but V_{Gj} was two times higher for the nozzle injection than that for the sinter injection. About 1.2 is generally recommended as C_0 for round pipes (Ishii 1977) and the value of 1.8 is fairly large. Kataoka & Ishii showed that C_0 was a function of pipe diameter and reached to about 1.8 in the pipe with diameter more than about 0.1 m based on the data by Ellis & Jones (1965). But they did not incorporate the effect of D_h into the final relation for C_0 and the value of C_0 of Kataoka's correlation is about 1.2 for this experiment. Since the larger C_0 means that the radial distribution of phase and/or velocity is steeper, the shape of the distribution in the large diameter pipe might be different from that in a small diameter pipe. As for the drift velocity, Kataoka & Ishii proposed a correlation from pool void fraction data under the wide range of experimental condition mentioned in Introduction. Figure 8 compares the data in this study with the correlation and another existing relations (Ishii 1977). The drift velocity for the sinter injection locates near the line of churn turbulent bubbly flow and that for the nozzle injection locates near the lines of maximum cap bubble and Kataoka's correlation. In the nozzle injection, some cap bubbles were clearly observed as described in the first section of this chapter and no such large bubbles were recognized in the sinter injection. The results in figure 8 corresponds to the flow observation results. Then, the

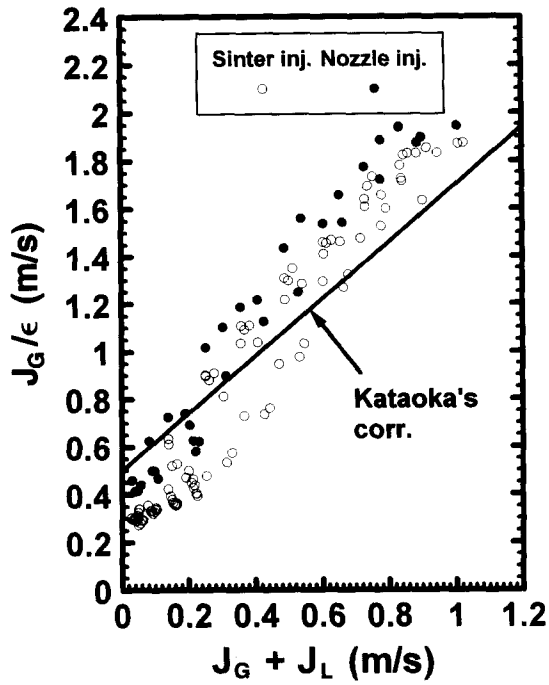

Figure 7. Comparison of drift–flux relations at top of test section with Kataoka's correlation.

difference of V_{Gj} between the mixing methods is supposed to be caused by the different size distribution of bubbles in the test section. The followings can be obtained from the comparisons with Kataoka's correlation;

(1) C_0 should be modeled including the effect of D_h and the radial distribution of phase and/or velocity might be steeper in the large D_h pipe,
(2) the bubble size distribution is affected by the air injection methods.

Hills (1976) proposed a relation between the relative velocity and the void fraction under J_L less than 0.3 m/s using data with D_h of 0.15 m and L/D_h of 70 in air–water system. Figure 9 compares the relation between the relative velocity V_r and ϵ. V_r at a ϵ is higher for the nozzle injection than that for the sinter injection and Hills' correlation underestimates V_r for the nozzle injection. In Hills' experiment, air was fed into the center of test section through a 0.051 m bore vertical pipe at the

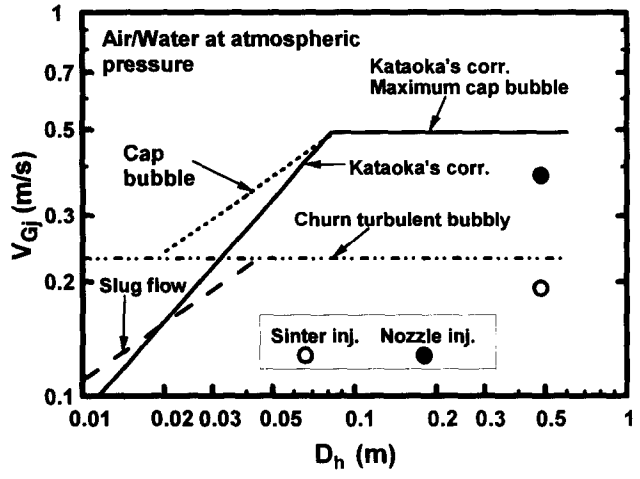

Figure 8. Comparison of drift velocity at top of test section with various relations and Kataoka's correlation.

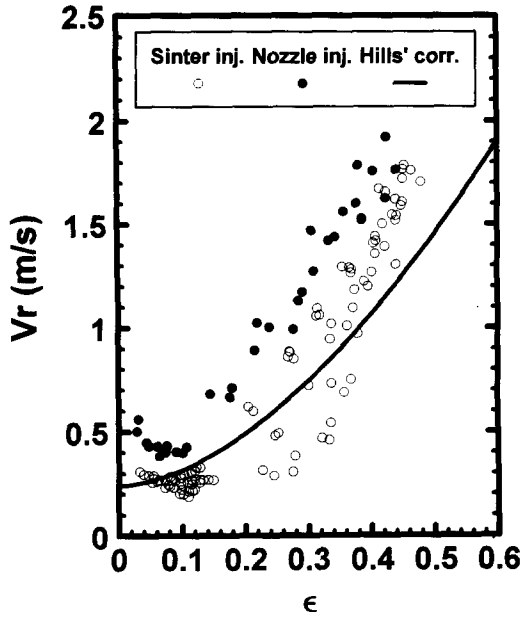

Figure 9. Comparison of relations of V_r and ϵ with Hills' correlation.

bottom of test section. The air injection method is similar to that of the nozzle injection in this study. However, the predictive accuracy is better for the sinter injection than that for the nozzle injection. The discrepancy between the present data in the nozzle injection and the correlation is supposed to be caused by the differences of D_h and/or L/D_h because the air injection method is similar and the fluid combination is the same each other. It was reported in Kataoka's paper (1987) that C_0 and V_{GJ} are almost constant for a pipe diameter greater than about 0.1 m. This means that the difference of L/D_h is supposed to cause the discrepancy. The cap bubbles in Hills' experiment might disintegrate to smaller bubbles through the large L/D_h test section. More studies are needed for the effect of L/D_h on the bubble size distribution to make clear the discrepancy between the present data in the nozzle injection and Hills' correlation.

4. CONCLUDING REMARKS

The flow structure in a developing air–water two-phase flow has been investigated experimentally along a large vertical pipe (D_h: 0.48 m, L/D_h: about 4.2). Two air injection methods (sinter injection and nozzle injection) were adopted to realize an extremely different flow structure in the developing region. The flow rate condition in the test section was as follows: J_G: 0.02–0.87 m/s (at atmospheric pressure) and J_L: 0.01–0.2 m/s, which covers the range of bubbly to slug flow in a small-scale pipe ($D_h \leqslant$ about 0.05 m). The measurement items were the flow pattern, the axial distribution of sectional differential pressure and the radial distribution of local void fraction. The sectional average void fraction at the top of the test section was compared with the previous correlations (drift–flux type Kataoka's correlation and Hills' correlation which gives the relation between V_r and ϵ). The following concluding remarks are derived from this study:

(1) no air slugs occupying the flow path are recognized in this experiment regardless of the air injection methods even under the condition where slug flow is realized in the small-scale pipe. The churn bubbly flow is observed under the condition except in the lower half of the test section in the nozzle injection where the disintegration of a large bubble to smaller bubbles is noticed,
(2) in the lower half of the test section, the axial distribution of sectional differential pressure and the radial distribution of local void fraction showed peculiar distributions depending on the air injection methods. However, in the upper half of the test section, the effects of the

air injection methods are small in respect of the shapes of the differential pressure distribution and the phase distribution,

(3) the comparison of sectional void fraction near the top of the test section with Kataoka's correlation indicated that C_0 of drift-flux model should be modeled including the effect of D_h and the bubble size distribution is affected by the air injection methods. The bubble size distribution is considered to be affected also by L/D_h based on the comparison of results with Hills' correlation.

REFERENCES

Ellis, J. E. & Jones, E. L. 1965 Vertical gas–liquid flow problems. *Symposium on Two-phase Flow*, Exeter, pp. B101–140.

Hills, J. H. 1974 Radial non-uniformity of velocity and voidage in a bubble column. *Transactions of the Institution of Chemical Engineers* **52,** 1–9.

Hills, J. H. 1976 The operation of a bubble column at high throughputs—I. Gas holdup measurements. *The Chemical Engineering Journal* **12,** 89–99.

Hashemi, A., Kim, J. H. & Sursock, J. P. 1986 Effect of diameter and geometry on two-phase flow regimes and carry-over in a model PWR hot leg. *Proceedings of The 8th International Heat Transfer Conference*, San Francisco, CA, pp. 2443–2451.

Ishii, M. 1977 One-dimensional drift-flux model and constitutive equations for relative motion between phases in various two-phase flow regimes. ANL-77-47.

Kataoka, I. & Ishii, M. 1987 Drift flux model for large diameter pipe and new correlation for pool void fraction. *International Journal of Heat and Mass Transfer* **30,** 1927–1939.

Liles, D. R., Spore, J. W., Knight, T. D., Nelson, R. A., Cappiello, M. W., Pasamehmetaglu, K. O., Mahaffy, J. H., Guffee, L. A., Stumpf, H. J., Dotson, P. J., Steinke, R. G., Shire, P. R., Greiner, S. E. & Sherwood, K. B. 1988 TRAC-PF1/MOD1 Correlations and Models. NUREG/CR-5069 LA-11208-MS.

Liu, T. J. & Bankoff, S. G. 1990 Structure of air–water bubbly flow in a vertical pipe: I—liquid mean velocity and turbulence measurements. *ASME FED-***99,** *HTD-***155,** 9–17.

Mishima, K. & Ishii, M. 1984 Flow regime transition criteria for upward two-phase flow in vertical tubes. *International Journal of Heat and Mass Transfer* **27,** 723–737.

Ohnuki, A., Akimoto, H. & Sudo, Y. 1995 Flow pattern and its transition in gas–liquid two-phase flow along a large vertical pipe. *Proceedings of The 2nd International Conference on Multiphase Flow '95—Kyoto*, Vol. 3, pp. FT1-17–FT1-23.

Ross, D. F. 1988 Compendium of ECCS research for realistic LOCA analysis. NUREG-1230.

Serizawa, A. & Kataoka, I. 1988 Phase distribution in two-phase flow. *Transient Phenomena in Multiphase Flow* (Edited by N. H. Afgan), pp. 179–224. Hemisphere Publishing Corp., New York.

Ueyama, K., Morooka, S., Koide, K., Kaji, H. & Miyauchi, T. 1980 Behavior of gas bubbles in bubble columns. *Ind. Eng. Chem. Process Des. Dev.* **19,** 592–599.